

Article

The Influence of Different Curing Environments on the Mechanical Properties and Reinforcement Mechanism of Dredger Fill Stabilized with Cement and Polypropylene Fibers

Ying Wang ¹ , Chaojie Wang ¹ , Zhenhua Hu ^{2,*}  and Rong Sun ²

¹ College of Transportation, Shandong University of Science and Technology, Qingdao 266590, China; wangying871209@sdust.edu.cn (Y.W.); 202183160020@sdust.edu.cn (C.W.)

² College of Civil Engineering and Architecture, Shandong University of Science and Technology, Qingdao 266590, China; 13789873609@163.com

* Correspondence: huzhenhua@sdust.edu.cn

Abstract: An effective method widely used in geotechnical engineering to solve the shrinkage and cracking issues in cement-stabilized soil (CS) is evenly mixing randomly distributed fibers into it. Dredger fills stabilized with cement and polypropylene fibers (PFCs) are exposed to rainwater immersion and seawater erosion in coastal areas, influencing their mechanical performance and durability. In this study, direct shear and consolidation compression tests were conducted to investigate the influence of different curing environments on the mechanical properties and compressive behavior of PFCs. Dominance and regression analyses were used to study the impact of each factor under different curing regimes. The reinforcement mechanism of different curing environments was also explored using scanning electron microscopy (SEM) imaging. The results show that the cohesion and elastic modulus of the specimens cured in seawater were reduced compared with those cured in freshwater and standard curing environments. The best fiber content for the strength and compressive modulus of PFCs was determined to be 0.9% of the mass of dredged fill. The results of value-added contributions and the relative importance of each factor in different curing environments show that the overall average contribution of cement content in the seawater curing environment is reduced by 6.79% compared to the freshwater environment. Multiple linear regression models were developed, effectively describing the quantitative relationships of different properties under different curing conditions. Further, the shear strength was improved by the coupling effect of soil particles, a C-S-H gel, and polypropylene fibers in the PFCs. However, the shear strength of the PFCs was reduced due to the structural damage of the specimens in the freshwater and seawater curing environments.

Keywords: stabilized soil; cement; polypropylene fiber; cohesion; compressive modulus; microstructure



Citation: Wang, Y.; Wang, C.; Hu, Z.; Sun, R. The Influence of Different Curing Environments on the Mechanical Properties and Reinforcement Mechanism of Dredger Fill Stabilized with Cement and Polypropylene Fibers. *Materials* **2023**, *16*, 6827. <https://doi.org/10.3390/ma16216827>

Academic Editor: Jacek Domski

Received: 20 September 2023

Revised: 18 October 2023

Accepted: 20 October 2023

Published: 24 October 2023



Copyright: © 2023 by the authors. Licensee MDPI, Basel, Switzerland. This article is an open access article distributed under the terms and conditions of the Creative Commons Attribution (CC BY) license (<https://creativecommons.org/licenses/by/4.0/>).

1. Introduction

Coastal reclamation has gained significant attention in recent years. However, dredger fill cannot be directly used for engineering applications due to its high moisture content, high compressibility, and low strength [1]. Therefore, different treatment methods have been proposed to improve the bearing capacity and shear strength of dredger fill. Adding stabilizers to dredger fill improves its mechanical properties [2–5]. Lime or cement are most commonly used as stabilizing agents. However, various issues associated with cement-stabilized soil (CS) hinder its applicability and prospect. CS can easily undergo shrinkage and cracking when dried due to highly dispersed inorganic colloids in the interior of the CS [6], leading to reduced stability and durability attributes. Compared with other stabilized soils, CS is prone to shedding, fragmentation, and other phenomena. At the same time, CS is inherently brittle under pressure, reducing the bearing capacity after the soil is destroyed [7]. These problems limit the further application and development of CS.

Fiber-reinforced soil is a composite soil in which a certain proportion of fibers are added to the soil to improve its physical and mechanical properties. Some researchers have confirmed that soil strength is improved by uniformly adding fibers because of the high strength and resistance to acid and alkali corrosion. Zhao et al. [8] used polypropylene fibers to stabilize natural sandy soils and studied the effect of different confining pressures, fiber amounts, and fiber lengths on the dynamic characteristics of the resulting fiber-reinforced soil through dynamic triaxial tests. Liu et al. [9] studied the durability of the cotton stalk fiber-reinforced soil and investigated the mechanism of cotton stalk fibers through single fiber tensile and scanning electron microscope tests. Jiang et al. [10] and Zhao et al. [11] studied the effects of fiber length and content on the shear strength behavior of the polypropylene fiber-reinforced soil.

In order to address the various issues associated with CS, several researchers have also attempted to improve CS's properties by incorporating it with fibers. Tiwari et al. [12], Akbari et al. [13], and Aryal et al. [14] used polypropylene fibers and cement as external additives to stabilize expansive soils, soft soils, and kaolin clays, respectively. It was confirmed that polypropylene fibers significantly increased CS's strength. Tan et al. [15] used coconut fibers treated by alkali activation and fly ash as external additives and proposed their beneficial use in effectively increasing soil strength and reducing the soil deformation capacity. Qiu et al. [16] quantitatively analyzed the effect of fiber content on soil stabilized by using carbon fibers as an external additive and stabilizing sand through microbial-induced calcite precipitation (MICP). Gobinath et al. [17] found that all the parameters of soil performance were enhanced by using banana fibers as an additive to improve soil stabilized by sodium carbonate. Cao et al. [18] studied the unconfined compressive strength (UCS) and microstructure of soils stabilized by basalt fibers, cement, and fly ash. Similarly, Hu et al. [19] evaluated the reinforcement mechanism of CS and alginate fibers and developed a compressive strength correction prediction model considering multiple parameters. In addition, Zhang et al. [20] used recycled GFRP (glass fiber-reinforced polymer) fibers and cement as additives and showed that the UCS of stabilized soil significantly increased when the fiber content was 5% of the wet soil mass.

In summary, improving the mechanical properties of dredger fill stabilized with cement and polypropylene fibers (PFCSs) is feasible. However, many factors can affect the resulting mechanical properties of PFCSs, especially when PFCSs are used in coastal areas where factors like precipitation and seawater erosion can influence their solidification. Hence, it is imperative to clarify the effect of different curing environments on the mechanical properties of PFCSs with various parameters before utilizing them for resource utilization. Based on these considerations, the effects of moisture content, polypropylene fiber content, cement content, and curing age on the shear strength and compression characteristics of PFCSs in different curing environments were studied in this paper through direct shear and consolidation compression tests. Furthermore, a dominance analysis was applied to analyze the impact of each factor on cohesion in different curing environments, and a regression analysis was used to establish linear equations between each factor and cohesion in different curing environments. Furthermore, SEM tests were conducted to analyze the reinforcement mechanism of PFCSs under different curing environments. These measures provide a scientific basis for resource utilization.

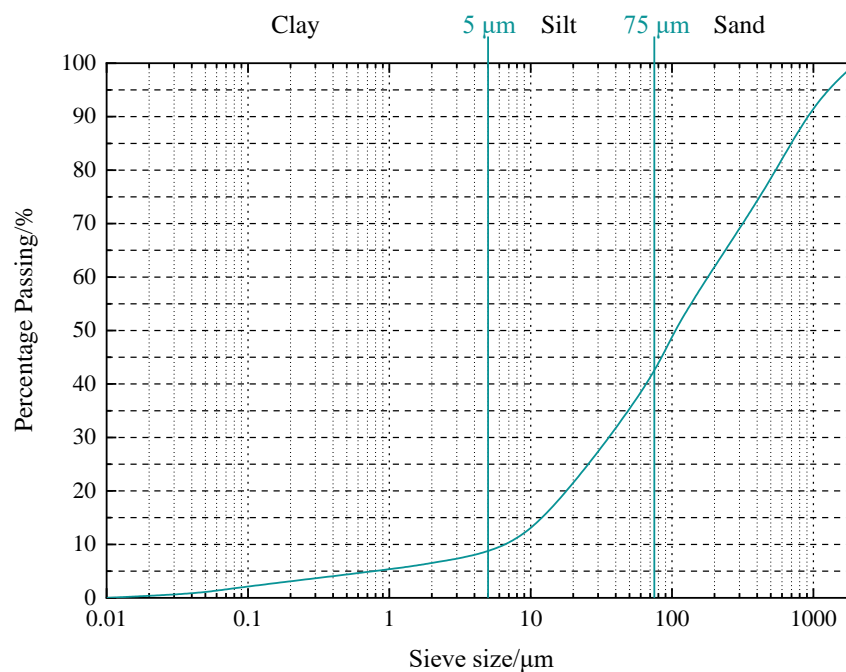
2. Raw Materials and Experimental Methods

2.1. Raw Materials

The soil used in this experiment was derived from the dredger fill of Xingguang Island in Qingdao. The basic physical properties of the dredger fill were determined following ASTM D854 [21], ASTM D4318 [22], ASTM D2216 [23], ASTM D7263 [24], and ASTM D2487 [25]. The basic physical characteristics of the dredger fill are listed in Table 1, while the particle size distribution (gradation) curve is shown in Figure 1.

Table 1. Basic physical characteristics of the dredger fill.

Specific Gravity	Water Content /%	Liquid Limit /%	Plastic Limit /%	Plasticity Index	Density /(g/cm ³)	Organic Matter /%
2.25	253.31	57.03	12.70	44.33	1.83	0.5

**Figure 1.** Grain size distribution curve of dredger fill.

In this study, polypropylene fibers and cement were used as stabilized agents to treat the dredger fill. The physical properties of the polypropylene fibers obtained from the manufacturer are given in Table 2. Cement-type PC 42.5 used in this study was produced by Anhui Conch Cement Co., Ltd., located in Anhui Province of China. The chemical composition of cement is presented in Table 3.

Table 2. Physical properties of polypropylene fibers.

Length /mm	Diameter /mm	Density /(g/cm ³)	Tensile Strength /MPa	Fracture Extension /%	Elastic Modulus /MPa
6	0.15	0.91	≥460	≥10	≥3500

Table 3. Compositions (wt.%) of cement.

SiO ₂	CaO	Fe ₂ O ₃	Al ₂ O ₃	Na ₂ O	K ₂ O	MgO	SO ₃	Others	Loss on Ignition
21.7	57.4	2.9	7.5	0.5	0.4	1.7	3.5	/	4.4

2.2. Sample Preparation

The experimental procedure is shown in Figure 2. First, the specimens were prepared according to the experimental procedure, followed by subjecting direct shear and consolidation compression tests. Finally, SEM imaging was performed on the specimens. Comprehensive details on the specific procedures and conditions used in these tests are provided in a later section.

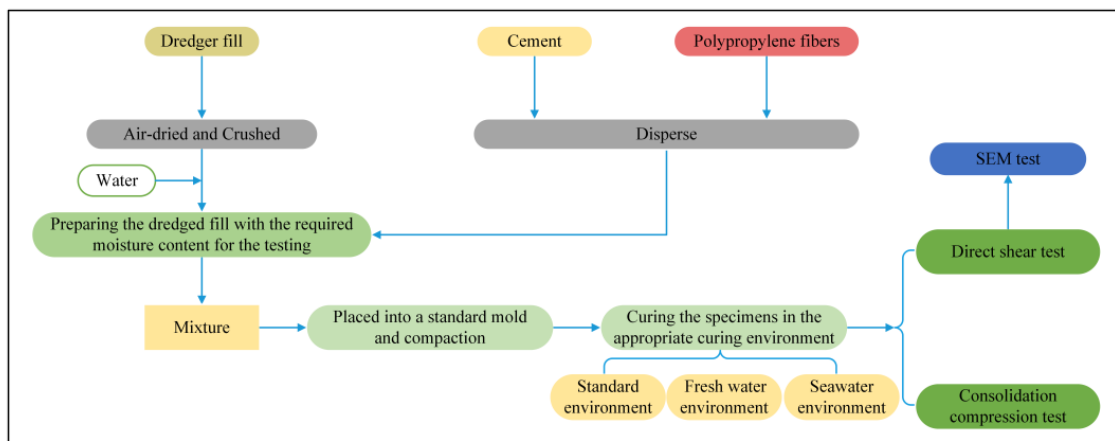


Figure 2. The experimental procedure.

2.3. Experimental Method

Direct shear tests were carried out to obtain the strength and deformation characteristics of PFCs in this study. In addition, one-dimensional consolidation tests were used to analyze the mechanical properties of PFCs. SEM imaging was conducted to study the strength and deformation characteristics.

In order to obtain the shear strength characteristics of PFCs, the direct shear test was conducted using a ZJ-type strain-controlled direct shear apparatus, following ASTM D3080 [26]. The specimens of the shear tests were subjected to three vertical pressures (100 kPa, 200 kPa, and 300 kPa). In this investigation, three samples were prepared for each mix, and the average was taken as the representative value. The average error was also obtained following each test. The test results were considered suitable if the average error was <5%. The specific test cases are listed in Table 4.

Table 4. Testing cases for direct shear test.

W/%	C/%	F/%	T/d	E
0.5 W _L	0	0, 0.6	0	-
0.5 W _L	6	0, 0.6, 0.9, 1.2	7	BC
0.5 W _L	6, 9, 12	0.6	7	WC, SC
0.5 W _L	6	0.6, 0.9, 1.2	7, 14, 28	WC, SC
0.75 W _L	6, 9, 12	0.9	7	WC, SC
1.0 W _L	6, 9, 12	0.9	7	WC, SC
1.5 W _L	6, 9, 12	0.9	7	WC, SC

Note: W represents the water content; C denotes the cement content; F represents the polypropylene fiber content; T is the curing time; E represents the curing environment; BC represents the standard curing environment; WC represents curing under a freshwater environment; SC represents curing in seawater.

In order to analyze the compressive behavior of PFCs, a consolidation compression test was carried out using a WG-type triaxial high-pressure single-lever consolidation apparatus based on ASTM D2435 [27]. During the consolidation compression test, loading was applied under 12.5, 25, 50, 100, 200, 300, 400, 800, and 1600 kPa. Each load level was kept stable for 24 h, with the test lasting 9 days. In this investigation, three samples were prepared from each mix. A series of cement contents (6% by weight of the wet soil), fiber contents (0.6%, 0.9%, or 1.2% by weight of the wet soil), a curing duration (7 days), and the curing environments (freshwater and seawater) were considered with a constant water content (1.0 W_L) of the dredger fill in this study.

In order to study the mechanism of the changes in the mechanical properties of PFCs from a microscopic perspective, SEM testing was conducted using the Nova NanoSEM450 scanning electron microscope instrument manufactured by FEI Company in Hillsboro, OR, USA. Specimens for SEM testing were taken from obvious locations of the failed sample,

and the specimen size was controlled to 5 mm × 5 mm × 5 mm to ensure consistency. The specimen was soaked in anhydrous ethanol under vacuum saturation for 48 h. Subsequently, the specimen was placed in a vacuum-drying oven at a suitable temperature to avoid damage to the specimen surface. Finally, the dried specimen was stored in a dry and well-ventilated place.

Secondary processing was performed on the specimen to control its size to 3 mm × 3 mm × 2 mm. The processed specimen was placed inside a vacuum sputter coater machine for gold coating. Then, the processed specimen with a thin gold film was transferred into the sample chamber of the SEM. The sample was observed under the microscope to observe its microstructure. An appropriate magnification was chosen during the observation to show the sample's microstructure adequately. An electron beam focused on the same spot for too long was avoided to prevent damaging the sample.

3. Results, Analysis, and Discussion

3.1. Mechanical Properties of PFCs

In order to characterize PFCs' shear strength, the cohesion and friction angle were obtained through direct shear tests [28,29]. In these tests, the change in the friction angle of each sample was insignificant, mainly concentrated between 10° and 20°. Hence, only the cohesion was analyzed in this paper in detail.

3.1.1. Cohesion of Different Specimens

The influence of different materials on the cohesion could be obtained by comparing the cohesion of different samples to carry out relevant research in the later stage. As shown in Figure 3, the highest cohesion was with PFCs, the second one was with CS, and the remolded soil had the least cohesion. The cohesion of the polypropylene fiber-reinforced soil increased by 47.55% compared with that of the remolded soil. Also, the cohesion of the CS increased by 350.40% compared with that of the remolded soil. The results indicate that soil cohesion was improved by adding polypropylene fibers or cement, and the effect of cement on cohesion improvement was higher than that of polypropylene fibers. Further, PFCs cohesion increased by 300.00% compared with the soil reinforced with polypropylene fibers and increased by 31.03% compared with the CS. Therefore, it can be inferred that the soil cohesion was improved more effectively by adding polypropylene fibers and cement.

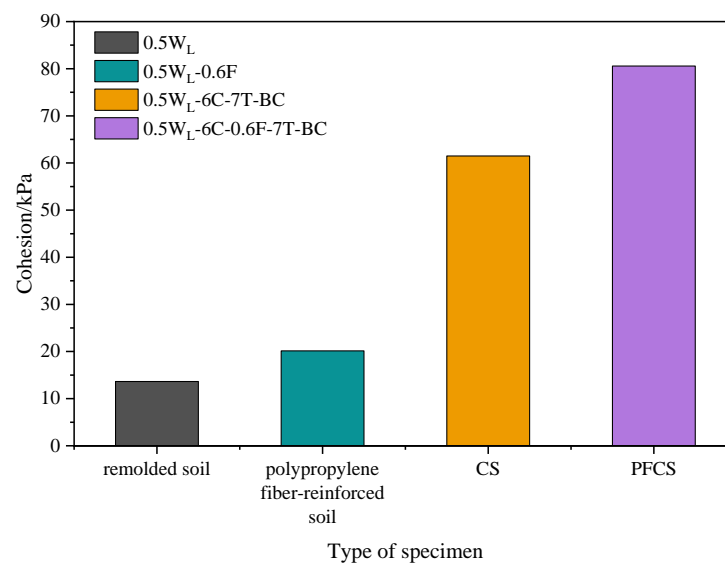


Figure 3. Cohesion of different specimens.

3.1.2. Cohesion of Different Curing Environments

The curing environment can alter the physical and chemical reactions in PFCs, significantly impacting its strength. Figure 4 shows that the cohesion in the standard curing

environment was highest, followed by that in the freshwater curing environment, while the lowest cohesion was observed for the specimens cured in seawater. Taking a polypropylene fiber content of 0.6% as an example, the cohesion of samples with a curing time of 7 d decreased by 3.95% in the freshwater curing environment and by 4.11% in the seawater curing environment, compared to that of samples cured under standard conditions. At 14 d and 28 d curing ages, the cohesion in the seawater curing environment decreased by 2.94% and 6.11%, respectively, compared with that in the freshwater curing environment. Similarly, the same declining pattern was exhibited for other polypropylene fiber contents. However, a polypropylene fiber content of 1.2% had a better effect.

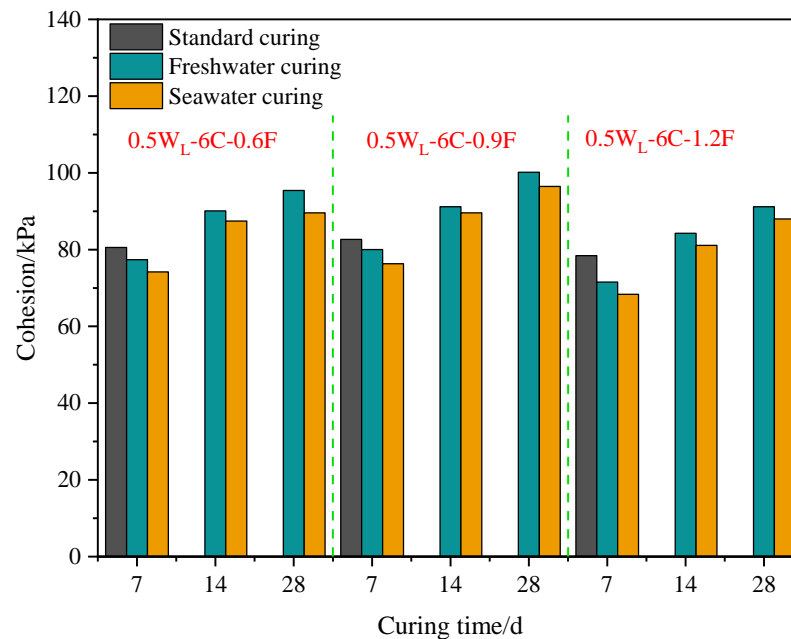


Figure 4. Cohesion of specimens with different curing environments.

The reduced cohesion observed in the specimens is because the soil had water absorption and swelling characteristics, and irregular deformation occurred when the sample was immersed in water. When this deformation exceeded the limit of the internal structure of the soil, microcracks appeared due to the stress concentration [1], damaging the internal structure of the soil. In the case of samples cured in a seawater environment, the main reason for the decrease in strength was attributed to the interference of seawater on the hydration reaction. Soaking any cementitious material in seawater causes the precipitation of calcium elements and Friedel's salt [30], destroying the C-S-H gel structure and generating pores in the sample.

3.1.3. Cohesion of Different Polypropylene Fiber Contents

Fiber content has a critical role in the enhancement of the mechanical behavior of composites. Figure 5 shows that the cohesion of the sample in a freshwater curing environment with a polypropylene fiber content of 0.9% increased by 3.42% compared with that of the sample with a polypropylene fiber content of 0.6% at a 7 d curing age. However, the cohesion strength of the sample with a polypropylene fiber content of 1.2% decreased by 10.60% compared to that of the sample with a polypropylene fiber content of 0.9%. Similarly, the same pattern of change was exhibited in both standard and seawater curing environments. This explains why PFCS cohesion first increased and then decreased with the increasing fiber content. Further, the sample with a polypropylene fiber content of 0.9% had the largest cohesion strength under different curing conditions.

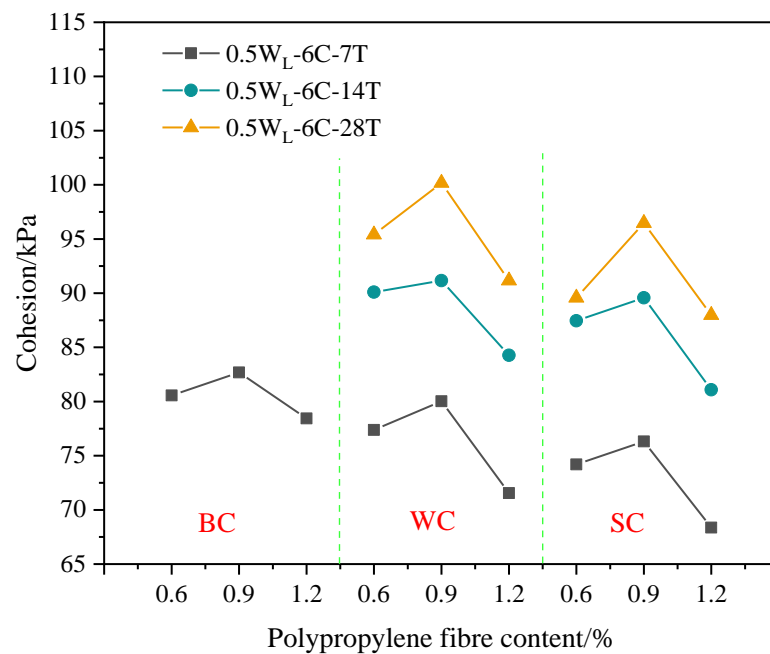


Figure 5. Cohesion of specimens with different polypropylene fiber contents.

This phenomenon is because the mechanism of polypropylene fibers was similar to that of plant roots reinforcing soil [31]. Based on this mechanism, it can be known that the CS pores were filled by polypropylene fibers, forming a denser structure of the PFCs. Meanwhile, frictional force was generated by the contact area between the polypropylene fiber and the mixed material particles based on friction theory when the PFCs were subject to a lateral load, which weakened the external load and suppressed the soil deformation [15]. However, when the polypropylene fiber content was greater than 0.9%, a negative effect on the improvement of the cohesion of the PFCs appeared by further increasing the polypropylene fiber content. A large amount of polypropylene fibers were difficult to distribute evenly in the PFCs, so fibers tended to form clusters and entangled with each other, damaging the overall structure of the soil [31]. Nevertheless, the main reason for the increase in cohesion of the CS was the production of C-S-H colloids [32], which could improve the overall integrity and performance of the soil. However, the too-high polypropylene fiber content could reduce the binding ability of cement, thus reducing the inter-particle interaction forces in the soil [33]. As shown in Figure 3, cement had a higher effect on improving cohesion than polypropylene fibers, which can macroscopically lead to a decreased cohesion of the PFCs. This also explains the increase of the reduced ratio in the freshwater and seawater environments with a fiber content of 1.2%, as shown in Figure 4.

3.1.4. Cohesion Due to Varying Cement Contents

Figure 6 shows that the cohesion of the sample in the freshwater curing environment linearly increased with the cement content. It also shows that the cohesion increased linearly with the cement content under seawater curing.

The main reason for this was that the C-S-H gel produced by the hydration reaction of cement possessed a bonding effect, which bonded together the soil particles in the PFCs [33]. Since the C-S-H gel structure is smaller than the soil particles, the pores of the particles were filled in the soil; hence, the soil structure was more compact, and finally, denser units were formed [33]. Also, the structure of the soil was more robust after the production of cement hydration products due to the higher strength of the C-S-H gel after hardening [34].

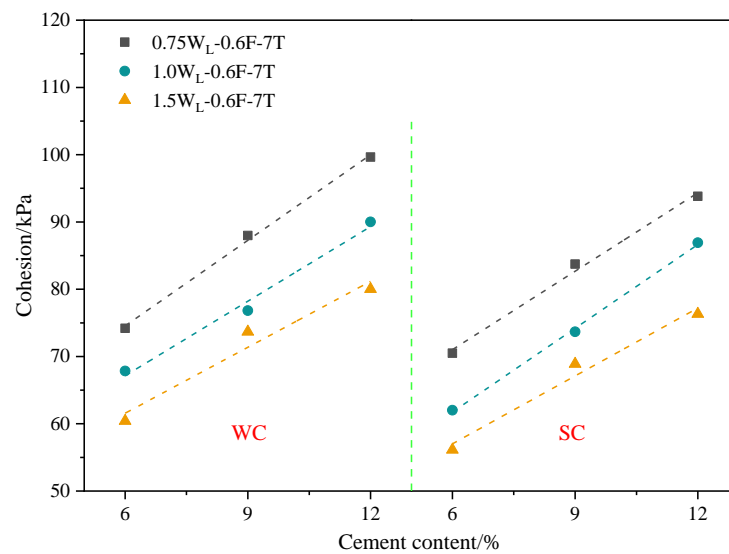


Figure 6. Cohesion of specimens with different cement contents.

3.1.5. Cohesion of Dredger Fill with Varying Moisture Contents

As shown in Figure 7, the cohesion of the sample in the freshwater curing environment with a moisture content of $1.0 W_L$ decreased by 8.57%, 12.67%, and 9.66%, respectively, compared with that of the sample with a moisture content of $0.75 W_L$ when cement contents were 6%, 9%, and 12%. The cohesion of the sample with a moisture content of $1.5 W_L$ decreased by 10.94%, 4.11%, and 11.09%, respectively, compared with that of the sample with a moisture content of $1.0 W_L$. Through the data, it is found that the cohesion decreased with the increase of the moisture content of the soil in the freshwater curing environment. This also reflects that the cohesion of the sample decreased with the increasing moisture content of the dredger fill in the seawater curing environments.

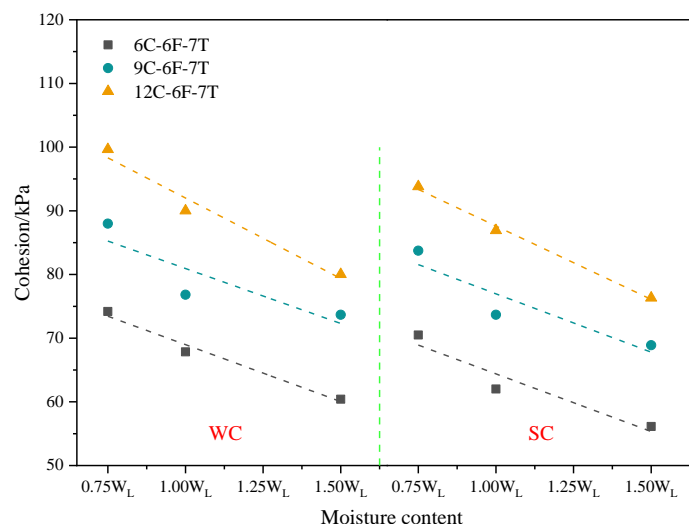


Figure 7. Cohesion of specimens with different moisture contents.

The internal interaction force between soil particles was van der Waals force [1], mainly composed of the molecular attraction of bonding material and bound water film. With the continuously increasing moisture content, the number of pores in the soil gradually increased, weakening the bonding effect between soil particles. Consequently, the van der Waals force decreased in the soil. In addition, a certain lubricating effect of water itself was possessed [30], and the increase in water content would expand this effect, making it easier for the soil to experience relative sliding under a lateral shear force.

3.1.6. Cohesion under Varying Curing Times

Figure 8 shows the cohesion results under varying curing times. When the polypropylene fiber contents were 0.6%, 0.9%, and 1.2%, the cohesion in the freshwater curing environment with a curing age of 14 d increased by 16.44%, 13.91%, and 17.78%, respectively, compared to that with a 7 d curing age. The cohesion with a curing time of 28 d increased by 5.88%, 9.88%, and 8.18%, respectively, compared to that with a curing time of 14 d. Similarly, the same pattern was exhibited in the seawater curing environment. It is also observed that the increasing cohesion with a curing time from 7 d to 14 d was greater than that from 14 d to 28 d, which is consistent with the findings of Deng et al. [35]. This is because the cohesion of PFCSs was affected by the curing time due to an increased cement hydration reaction. As the curing time increased, cement hydration further progressed. Although the C-S-H gel continued to be produced, the yield gradually decreased, resulting in a smaller improvement in the cohesion strength of the sample.

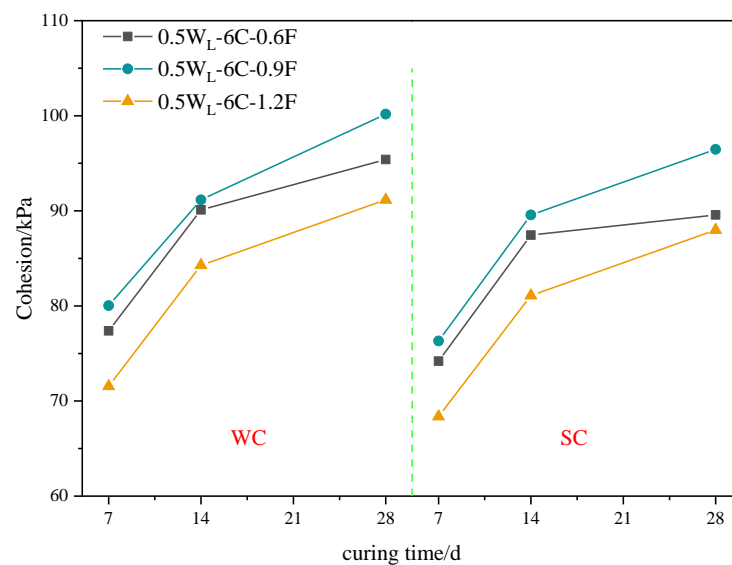


Figure 8. Cohesion of specimens with different curing times.

3.2. Compressive Properties of PFCSs

Foundation settlement is an important indicator for describing foundation deformation. When the stabilized soil of the dredger fill is directly used as a filling material, it is imperative to obtain the compression indicators of the stabilized soil to evaluate the foundation settlement. Therefore, the compression indicators of PFCSs should be calculated first before practical engineering applications.

3.2.1. Compression Curves of PFCSs

Figure 9 shows that the specimen with a polypropylene fiber content of 0.9% exhibited optimal compressive properties in freshwater and seawater curing environments. The specimen without polypropylene fiber had the poorest compressive properties. The decrease in the void ratio with PFCSs was mainly due to the spatial network structure and bridging effect [36] formed by the polypropylene fibers inside the sample. Further, the sample with a polypropylene fiber content of 0.9% had the best reinforcement effect, validating the results in Figure 5. Also, the void ratio of specimens cured in a freshwater environment was higher than those cured in a seawater environment under the same conditions. This might be because the hydration reaction can be interfered with and damaged in the seawater environment, leading to erosion and the swelling effect of dredger fill's water absorption. This is consistent with the results presented in Figure 4.

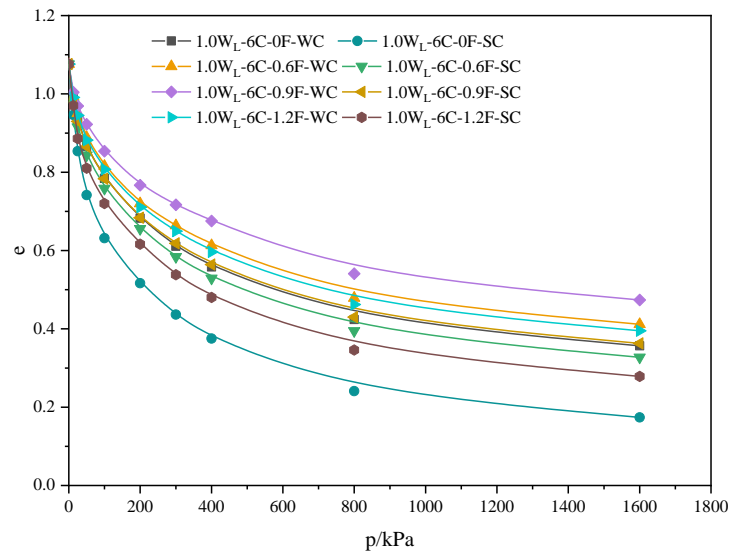


Figure 9. Compression curves of different specimens.

3.2.2. Compressive Modulus of PFCs

As shown in Figure 10, the compressive modulus increased initially and then decreased with the increasing content of fibers. The largest compressive modulus of specimens was obtained for 0.9% of polypropylene fiber content, while the smallest compressive modulus was observed for the samples without any polypropylene fiber content. Taking the freshwater curing environment as an example, the compressive modulus of samples with 0.9% of polypropylene fiber content increased by 21.21% than those without any polypropylene fiber content. This result further confirms that the compressive modulus was reduced by adding polypropylene fibers into CS and proved that the best reinforcement effect of the CS improved by fibers could be provided with 0.9% of polypropylene fiber content.

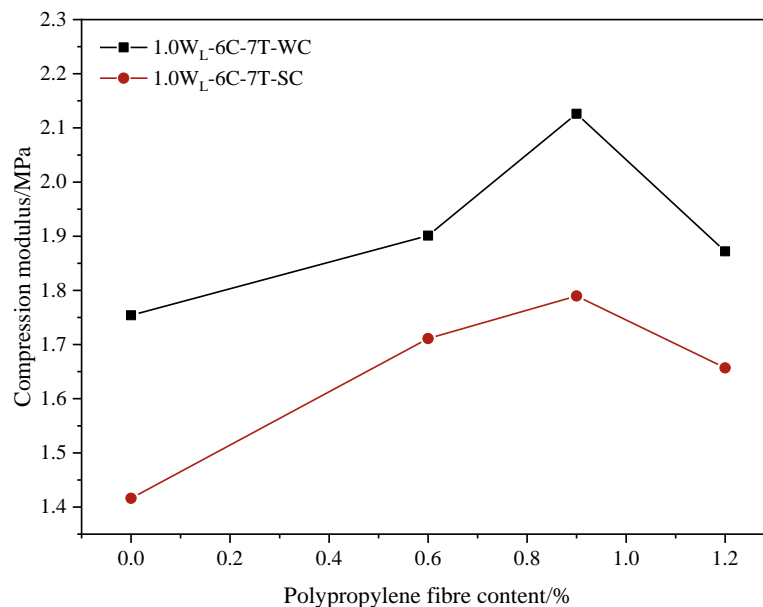


Figure 10. Compressive modulus of samples with different polypropylene fiber contents.

Meanwhile, it can be observed that under the same conditions in Figure 10, the compressive modulus of the samples cured in a freshwater environment was higher than that of the samples cured in a seawater environment. When the polypropylene fiber content was 0.9%, the compressive modulus of the samples cured in a freshwater environment

increased by 18.81% compared to those cured in a seawater environment. This result can further validate the findings given earlier in Figure 4.

3.3. Analysis and Discussion

1. Comparing the cohesion of four soils, the highest cohesion was found for PFCs, followed by CS, while the remolded soil had the lowest cohesion strength. The soil cohesion improved more effectively by synergistically adding polypropylene fibers and cement.
2. For different curing environments, the cohesion of the specimens cured in a standard curing environment was improved by 4.11% compared with those cured in a freshwater curing environment, while those cured in a freshwater curing environment were improved by 3.03–6.51% compared with those cured in a seawater curing environment, and the compressive modulus of the specimens cured in a seawater curing environment was reduced by 18.81% compared to that of the samples cured in a freshwater environment.
3. The mechanical properties and compressive behavior of PFCs were studied under different curing environments. The cohesion was improved by adding polypropylene fibers into CS, and the compressibility was also reduced effectively. The best polypropylene fiber content was determined to be 0.9%. The cohesion of PFCs increased with the increasing cement content and curing time but decreased with the increase of moisture content.

4. Experimental Data Analysis

4.1. The Dominance Analysis Method

4.1.1. Correlation Analysis

In order to conduct a correlation analysis on the cohesion of PFCs, four influencing factors were selected, i.e., moisture content, polypropylene fiber content, cement dosage, and curing time. In a freshwater curing environment, the correlation coefficients between the four factors and cohesion were 0.494, 0.104, 0.281, and 0.623, whereas, under seawater curing, the correlation coefficients between the four factors and cohesion were 0.521, 0.109, 0.258, and 0.616. From the correlation coefficients, it is observed that the four influencing factors have an impact on cohesive strength. Among them, the curing time has the highest influence on cohesion, while the polypropylene fiber content has the least impact.

4.1.2. Qualitative Analysis of Advantages

The dominance analysis method was used to assess the impact of each factor on cohesion. The dominance relationship in the dominance analysis method can be divided into complete dominance and general dominance levels. Complete dominance is the condition in which the relative importance sequence of each predictor variable is constant across all sub-models. General dominance refers to the relative importance sequence of predictor variables under the overall average contribution.

Four influencing factors (moisture content, X_1 ; polypropylene fiber content, X_2 ; cement content, X_3 ; and curing time, X_4) on cohesion as the dependent variable were selected, and the changes in the correlation coefficients were calculated when each influencing factor was included in separate sub-models without considering its influence. The change in correlation coefficient could represent the contribution of each influencing factor in terms of value added. The average value of the value-added contribution also represented the advantage weight (average contribution) of these influencing factors. The relation for calculating is given as Equation (1).

$$C_{X_i}^{(k)} = (\sum R_{yX_h X_i}^2) / (k^P - 1) \quad (1)$$

where $C_{X_i}^{(k)}$ is the average contribution of a variable when k influencing factors are contained in a sub-model, and this average contribution is with respect to the dependent variable y ;

$R_{y \times X_h X_i}^2$ is the change in correlation coefficient when a variable is added to a sub-model with k influencing factors; X_h is the k influencing factors; P is the number of influencing factors; and k is the number of influencing factors ($k = 0, \dots, P - 1$).

The relation for the total average contribution of influencing factors on cohesion is given by Equation (2).

$$C_{X_i} = \frac{1}{P} \sum_{k=0}^{P-1} C_{X_i}^{(k)} \tag{2}$$

The magnitude of the total average contribution of each influencing factor could reflect its respective importance. According to Equations (1) and (2), the incremental contribution and total average contribution of the four influencing factors (moisture content, X_1 ; polypropylene fiber contents, X_2 ; cement contents, X_3 ; and curing time X_4) on cohesion were calculated in the freshwater curing environment. The results are listed in Table 5.

Table 5. Value-added contribution and total average contribution of each influencing factor on cohesion in the freshwater curing environment.

Variables in the Model	Contribution	Value-Added Contribution			
		X_1	X_2	X_3	X_4
When K = 0, the average contribution	0	0.234	0.011	0.079	0.388
X_1	0.243	-	0.013	0.368	0.204
X_2	0.011	0.245	-	0.073	0.378
X_3	0.079	0.532	0.005	-	0.566
X_4	0.388	0.059	0.001	0.257	-
When K = 1, the average contribution	0.279	0.279	0.006	0.233	0.383
$X_1 X_2$	0.256	-	-	0.356	0.193
$X_1 X_3$	0.611	-	0.001	-	0.286
$X_1 X_4$	0.447	-	0.002	0.450	-
$X_2 X_3$	0.084	0.528	-	-	0.565
$X_2 X_4$	0.389	0.060	-	0.260	-
$X_3 X_4$	0.645	0.252	0.004	-	-
When K = 2, the average contribution	0.280	0.280	0.002	0.355	0.348
$X_1 X_2 X_3$	0.612	-	-	-	0.288
$X_1 X_2 X_4$	0.449	-	-	0.451	-
$X_1 X_3 X_4$	0.897	-	0.003	-	-
$X_2 X_3 X_4$	0.649	0.251	-	-	-
When K = 3, the average contribution	0.251	0.251	0.003	0.451	0.288
$X_1 X_2 X_3 X_4$	0.900	-	-	-	-
Total average contribution		0.263	0.006	0.280	0.352
Percentage		29.24%	0.63%	31.06%	39.07%

In a freshwater curing environment, the magnitude order of the four factors influencing the cohesion of the specimens was curing time > cement content > water content > polypropylene fiber content.

From the complete dominance and general dominance perspectives, the value-added contributions for six pairs of variables (X_1 versus X_2 , X_1 versus X_3 , X_1 versus X_4 , X_2 versus X_3 , X_2 versus X_4 , and X_3 versus X_4) were compared by analyzing the data in Table 5. The results with non-empty value-added contributions were produced as follows: X_1 had a complete advantage over X_2 , X_4 had a complete advantage over X_1 , X_3 had a complete advantage over X_2 , X_4 had a complete advantage over X_2 , X_3 had a general advantage over X_1 , and X_4 had a general advantage over X_3 .

Based on Equations (1) and (2), the calculation of the incremental and total average contributions of four influencing factors (moisture content, X_1 ; polypropylene fiber content, X_2 ; cement content, X_3 ; and curing time, X_4) on cohesion in the seawater curing environment are presented in Table 6.

Table 6. Value-added contribution and total average contribution of each influencing factor on cohesion in the seawater curing environment.

Variables in the Model	Contribution	Value-Added Contribution			
		X ₁	X ₂	X ₃	X ₄
When K = 0, the average contribution	0	0.270	0.012	0.066	0.379
X ₁	0.270	-	0.015	0.355	0.186
X ₂	0.012	0.273	-	0.060	0.368
X ₃	0.066	0.559	0.006	-	0.543
X ₄	0.379	0.077	0.001	0.230	-
When K = 1, the average contribution		0.303	0.007	0.215	0.366
X ₁ X ₂	0.285	-	-	0.341	0.174
X ₁ X ₃	0.625	-	0.001	-	0.262
X ₁ X ₄	0.456	-	0.003	0.431	-
X ₂ X ₃	0.072	0.554	-	-	0.540
X ₂ X ₄	0.380	0.079	-	0.232	-
X ₃ X ₄	0.609	0.278	0.003	-	-
When K = 2, the average contribution		0.304	0.002	0.355	0.325
X ₁ X ₂ X ₃	0.626	-	-	-	0.263
X ₁ X ₂ X ₄	0.459	-	-	0.430	-
X ₁ X ₃ X ₄	0.887	-	0.002	-	-
X ₂ X ₃ X ₄	0.612	0.277	-	-	-
When K = 3, the average contribution		0.277	0.002	0.430	0.263
X ₁ X ₂ X ₃ X ₄	0.899	-	-	-	-
Total average contribution		0.288	0.006	0.261	0.333
Percentage		32.44%	0.67%	29.41%	37.49%

For the perspective of relative importance in Table 6, it can be observed that in the seawater curing environment, the order of the magnitude of the impact of the four factors on cohesion was curing time > moisture content > cement content > polypropylene fiber content. Compared with the results obtained for the freshwater curing environment, the impact of cement content was reduced under the seawater curing environment.

Similarly, the comparison results with non-empty value-added contributions from complete dominance and general dominance perspectives were represented as follows: X₁ had a complete advantage over X₂; X₃ had a complete advantage over X₂; X₄ had a complete advantage over X₂; X₁ had a general advantage over X₃; X₄ had a general advantage over X₁; and X₄ had a general advantage over X₃. Compared with the results of value-added contributions in the freshwater curing environment, the opposing trend was reflected in the value-added contributions for X₁ and X₃, indicating that the effect of cement content was reduced. The comparison results were consistent with the results of relative importance.

The influence of cement content was reduced in the seawater curing environment compared with that in the freshwater curing environment. This is because the main chemical composition of ordinary Portland cement in the seawater environments has CaO, SiO₂, Al₂O₃, Fe₂O₃, and SO₂. The main ions eroded by seawater are Mg²⁺, Cl⁻, and SO₄²⁻. First, Mg²⁺ ions reacted with cement soil to form MgO · SiO₂ · H₂O, and 3CaO · SiO₂ · 2H₂O was dispersed, reducing the cementitious properties, thus lowering the strength of the stabilized soil.

4.2. Regression Analysis

4.2.1. Mathematical Modeling

A regression analysis was conducted to establish the quantitative relationship between cohesion and the influencing factors to analyze the influence of various factors on the cohesion of PFCs in freshwater and seawater curing environments. Hence, a multiple linear model was developed among the cohesion, moisture content, polypropylene fiber content, cement content, and curing time.

Based on the experimental data, a multiple linear regression analysis was conducted on the test results using IBM SPSS Statistics for Windows, Version 27.0 (IBM Corp., Armonk, NY, USA). The results are listed in Tables 7–9.

Table 7. The phase of the relationship results.

Correlation Coefficient	Coefficient of Determination	Adjusted Coefficient of Determination	Standard Error of Estimate
0.950	0.902	0.877	3.982

Table 8. Analysis of variance results.

Model	Sum of Squares	Degrees of Freedom	Mean Square	F-Test Statistic	Significance
Regression	2324.540	4	581.135	36.642	0.001
Residuals	253.759	16	15.860		
Sum	2578.299	20			

Table 9. The regression equation coefficient and inspection results.

Model	Partial Regression Coefficient		Standardized Partial Regression Coefficient	Independent Variable Test Statistic	Significance
	Regression Coefficient	Standard Error			
Constant	60.202	5.188		11.604	0.001
W	−0.348	0.054	−0.618	−6.408	0.001
F	−3.469	4.646	0.060	−0.747	0.466
C	4.018	0.469	0.792	8.572	0.001
T	0.920	0.135	0.610	6.820	0.001

Based on the coefficients in Table 9, the four-variable linear regression equation for the cohesion of the test samples in the freshwater curing environment was expressed as Equation (3).

$$c = 60.202 - 0.348W - 3.469F + 4.018C + 0.920T \quad (3)$$

where c is cohesion (kPa); W is the moisture content (%); F is the polypropylene fiber content (%); C is the cement content (%); and T is the curing time (d).

In order to better quantify the impact of freshwater and seawater curing environments on the cohesion of PFCSs, a reduction formula is defined as given in Equation (4).

$$\eta = \frac{c_s}{c_w} \quad (4)$$

where η is the reduction coefficient; c_s is the cohesion of the samples in the seawater curing environment (kPa); and c_w is the cohesion of the samples in the freshwater curing environment (kPa).

The cohesion of the soil samples under both curing environments was studied by analyzing experimental data to calculate the reduction coefficient. The average of these reduction coefficients was taken as the overall reduction coefficient in this study. Thus, the overall reduction coefficient was determined to be 0.953 from Equation (4). The four-variable linear regression equation for the cohesion of the samples in the seawater curing environment with various influencing factors is given in Equation (5).

$$c = 0.953 \times (60.202 - 0.348W - 3.469F + 4.018C + 0.920T) \quad (5)$$

4.2.2. Model Validation

The experimental results were validated to corroborate the reliability of the regression equation. The experimental values and predicted values of the cohesion of the samples in the freshwater and seawater curing environments are presented in Tables 10 and 11.

Table 10. The experimental results and predicted values of the samples in the freshwater environment and their errors.

W	F	C	T	Cohesion			
				Experimental Values /kPa	Predicted Values /kPa	Residuals /kPa	Relative Error
28.52	0.60	6.00	7	77.38	78.75	−1.37	−1.76%
28.52	0.90	6.00	7	80.03	77.70	2.33	2.91%
28.52	1.20	6.00	7	71.55	76.66	−5.11	−7.15%
28.52	0.60	6.00	14	90.10	85.19	4.91	5.45%
28.52	0.90	6.00	14	91.16	84.14	7.02	7.70%
28.52	1.20	6.00	14	84.27	83.10	1.17	1.38%
28.52	0.60	6.00	28	95.40	98.07	−2.67	−2.79%
28.52	0.90	6.00	28	100.17	97.02	3.15	3.14%
28.52	1.20	6.00	28	91.16	95.98	−4.82	−5.29%
28.52	0.60	6.00	7	77.38	78.75	−1.37	−1.76%
43.97	0.60	6.00	7	70.49	73.37	−2.88	−4.08%
55.03	0.60	6.00	7	64.13	69.52	−5.39	−8.40%
42.77	0.90	6.00	7	74.20	72.74	1.46	1.96%
55.03	0.90	6.00	7	67.84	68.48	−0.64	−0.94%
85.85	0.90	6.00	7	60.42	57.75	2.67	4.41%
42.77	0.90	9.00	7	87.98	84.80	3.18	3.62%
55.03	0.90	9.00	7	76.83	80.53	−3.70	−4.82%
85.85	0.90	9.00	7	73.67	69.81	3.86	5.24%
42.77	0.90	12.00	7	99.64	96.85	2.79	2.80%
55.03	0.90	12.00	7	90.01	92.58	−2.57	−2.86%
85.85	0.90	12.00	7	80.03	81.86	−1.83	−2.29%

Table 11. The experimental results and predicted values of the samples in the seawater environment and their errors.

W	F	C	T	Cohesion			
				Experimental Values /kPa	Predicted Values /kPa	Residuals /kPa	Relative Error
28.52	0.60	6.00	7	74.20	75.02	−0.82	−1.10%
28.52	0.90	6.00	7	76.32	74.02	2.30	3.01%
28.52	1.20	6.00	7	68.37	73.03	−4.66	−6.82%
28.52	0.60	6.00	14	87.45	81.15	6.30	7.20%
28.52	0.90	6.00	14	89.57	80.16	9.41	10.51%
28.52	1.20	6.00	14	81.09	79.17	1.92	2.37%
28.52	0.60	6.00	28	89.57	93.42	−3.85	−4.30%
28.52	0.90	6.00	28	96.46	92.43	4.03	4.18%
28.52	1.20	6.00	28	87.98	91.44	−3.46	−3.93%
28.52	0.60	6.00	7	74.2	75.02	−0.82	−1.10%
43.97	0.60	6.00	7	68.37	69.89	−1.52	−2.22%
55.03	0.60	6.00	7	59.39	66.22	−6.83	−11.51%
42.77	0.90	6.00	7	70.49	69.30	1.19	1.69%
55.03	0.90	6.00	7	62.01	65.23	−3.22	−5.20%
85.85	0.90	6.00	7	56.13	55.02	1.11	1.98%
42.77	0.90	9.00	7	83.74	80.78	2.96	3.53%
55.03	0.90	9.00	7	73.67	76.72	−3.05	−4.13%
85.85	0.90	9.00	7	68.90	66.50	2.40	3.48%
42.77	0.90	12.00	7	93.81	92.26	1.55	1.65%
55.03	0.90	12.00	7	86.92	88.20	−1.28	−1.47%
85.85	0.90	12.00	7	76.32	77.98	−1.66	−2.18%

In regression analysis, the error ratio and small error probability are important indicators for testing the model accuracy. The calculation equation is given as Equation (6).

$$C = \frac{S_2}{S_1} \quad (6)$$

$$P = \left\{ \left| \left(\varepsilon^{(0)}(t) - \bar{\varepsilon}^{(0)} \right) \right| < 0.6745S_1 \right\} \quad (7)$$

where C is the error ratio; S_1 is the mean squared deviation of the observed values; S_2 is the mean squared deviation of the residual sequence; P is the small error probability; $\varepsilon^{(0)}(t)$ is the residual values (kPa); and $\bar{\varepsilon}^{(0)}$ is the mean of the residuals (kPa).

The grey forecasting accuracy test criteria are presented in Table 12.

Table 12. The GM (1,1) grey forecasting precision inspection standard.

Standard	C	P
Good	<0.35	>0.95
Qualified	<0.50	>0.80
Pass with difficulty	<0.65	>0.70
Unqualified	≥0.65	≤0.71

It is found that the coefficient C in Equation (3) is 0.31 and P is 1.00 by calculating using Equations (6) and (7). For Equation (5), the coefficient C is 0.34 and P is 0.95. This indicates that Equations (3) and (5) can effectively describe the quantitative relationship between the cohesion and moisture content, polypropylene fiber content, cement content, and curing time in freshwater and seawater curing environments.

5. Microscopic Mechanism of PFCSs

The polypropylene fibers were randomly distributed in the CS, forming a spatial mesh structure, as shown in Figure 11. Since fibers cannot participate in cement hydration reactions, the relative frictional force provided by the rough surface of the fiber enhanced the PFCSs' cohesion [36,37]. Further, the polypropylene fibers limit particle movement and suppress cracks effectively [36,38]. In addition, a larger surface area for attaching to the C-S-H gel and soil particles was generated in the fiber with a rough surface, compensating for density reduction caused by fiber bonding. Inside the PFCSs, a mutual coupling effect existed between soil particles, the C-S-H gel, and polypropylene fibers—C-S-H gel-bonded soil particles and polypropylene fibers together, allowing for loose soil to aggregate and increasing internal stability and reducing its deformation capacity. Meanwhile, the C-S-H gel produced by the hydration reaction covered the fiber surface, making their surface rougher and increasing the frictional force between the fibers and soil particles. This significantly enhanced the ability of the polypropylene fibers to capture soil particles. Finally, a more solid overall structure inside the soil was formed by connecting the larger soil particles with better bonding to the less cohesive soil particles, reducing the deformation in the stabilized soil.

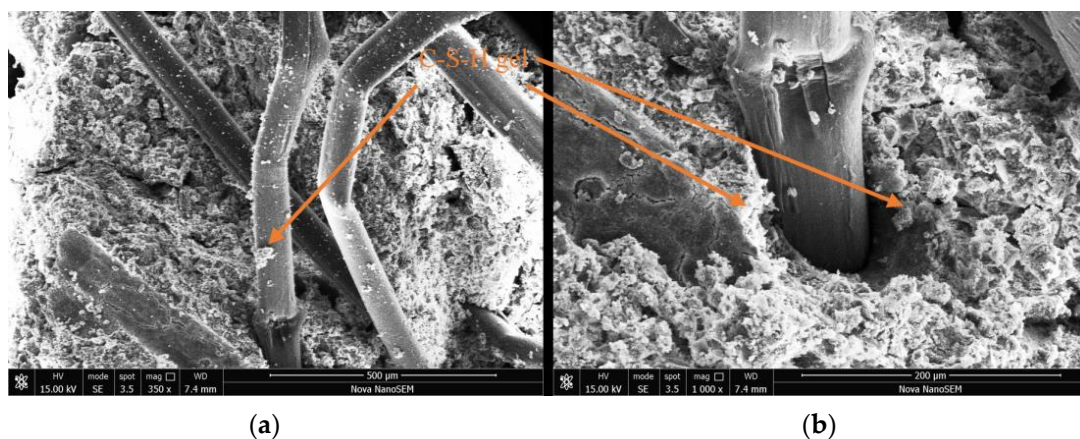


Figure 11. SEM images of PFCSs: (a) $\times 350$, (b) $\times 1000$.

Figure 12a,b show that the larger volumes of mixed particles comprising soil particles and the C-S-H gel were exhibited in the specimens cured in the freshwater curing environment compared with the specimens in the standard curing environment, so a greater C-S-H gel was required to encapsulate and connect these aggregates. In this case, some aggregates could not be adequately connected to neighboring aggregates, resulting in weak internal structures within the specimens. Hence, the failure and deformation of specimens may occur due to these weak structures. Additionally, this shows that a denser structure can be produced by closely connecting the aggregates on the surface of specimens in the standard curing environment. In contrast, noticeable cracks between the aggregates were exhibited in specimens cured in a freshwater curing environment. These cracks reduced the ability of PFCSs to resist deformation. As shown in Figure 12c, it can be proposed that the relatively smooth C-S-H gel with only a small amount of distribution appeared in seawater curing environments compared with the specimens cured in standard and freshwater environments, and the specimens in seawater curing environments showed a higher presence of densely distributed microcracks internally. In addition, the main reason for the increased strength of the PFCSs was the formation of a C-S-H gel [33]. However, the overall density within the PFCSs in seawater curing environments was reduced due to the decrease in the number of C-S-H-gel formations and microcracks, which decreased the mechanical performance.

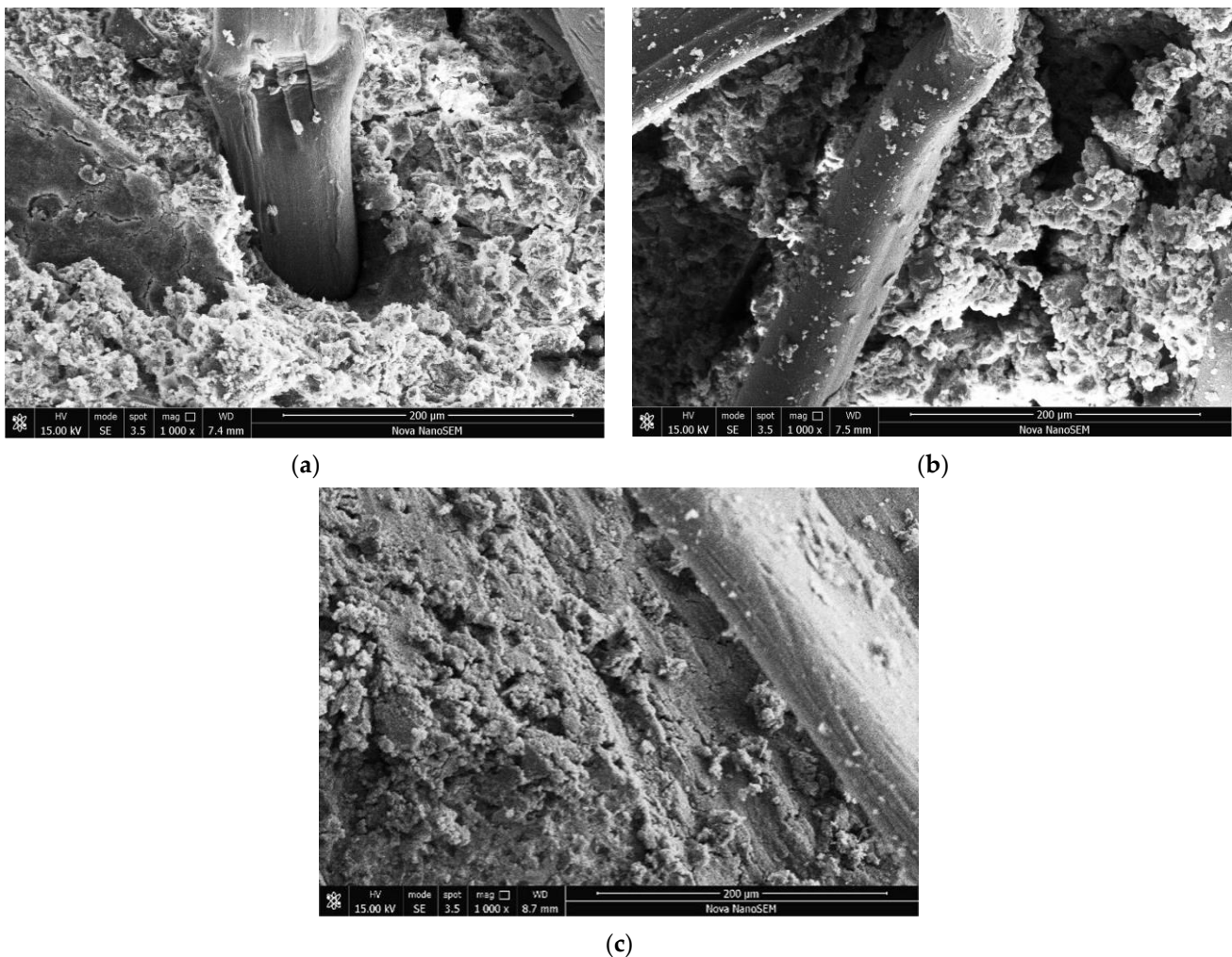


Figure 12. SEM images of PFCSs with different curing environments: (a) Standard curing environment. (b) Freshwater curing environment. (c) Seawater curing environment.

6. Conclusions

In this study, the mechanical and compressive properties of PFCSs were analyzed through direct shear and consolidation compression tests with different curing environments. The impact of each factor in the different curing environments was analyzed by the dominance analysis and regression analysis, and the microscopic mechanism was explored by SEM imaging. The main conclusions drawn from the obtained results are as follows.

1. The improvement of soil cohesion by adding polypropylene fibers and cement was more pronounced. The cohesion of the specimens cured under the standard curing environment was improved by 4.11% compared with those cured in the freshwater curing environment, whereas those cured in the freshwater curing environment were improved by 3.03–6.51% compared with those cured in the seawater curing environment. PFCS cohesion increased with the cement content and curing time but decreased with the increasing moisture content. The compression behavior of PFCSs was analyzed through consolidation testing, and the compressive modulus of the specimens cured in the seawater curing environment was reduced by 18.81% compared to those cured in the freshwater environment. The best polypropylene fiber content in direct shear and consolidation specimens was 0.9%.
2. The impact of each factor on cohesion was analyzed by the dominance analysis method. Comparing the results of value-added contributions and the relative importance of the specimens in freshwater and seawater curing environments, the results indicate that the impact of cement content had been reduced in the seawater curing environment. In addition, multiple linear regression models were established in freshwater and seawater curing environments, and the models can effectively describe the quantitative relationship between the cohesion and moisture content, polypropylene fiber content, cement content, and curing time in both freshwater and seawater curing environments.
3. A unique network structure formed by adding polypropylene fibers into CS was observed through SEM tests. The synergistic action with the C-S-H gel, soil particles, and polypropylene fibers improved the overall structural stability of the PFCSs. Compared to the standard-cured specimens, the larger aggregate volumes and noticeable cracks of freshwater-cured specimens were produced at the aggregate–binder interface. The amount of C-S-H gel formed was significantly lower in seawater-cured specimens than in the standard-cured and freshwater-cured specimens. The microscopic structural characteristics contribute to the decreased mechanical properties of PFCSs.

Author Contributions: Theoretical analysis, Y.W.; theory and methodology, Y.W. and Z.H.; writing—reviewing and editing, Y.W. and R.S.; testing and data analysis, C.W.; writing—original draft preparation, C.W.; conceptualization, Z.H.; data curation, Z.H. All authors have read and agreed to the published version of the manuscript.

Funding: The authors gratefully acknowledge the financial support from the Shandong Province Natural Science Foundation (Grant No: ZR2021ME067, ZR2023ME038) and the Youth Innovation Technology Project of Higher School in Shandong Province (Grant No: 2022kj217).

Institutional Review Board Statement: Not applicable.

Informed Consent Statement: Not applicable.

Data Availability Statement: Not applicable.

Conflicts of Interest: The authors declare no conflict of interest.

References

1. Zhang, X.; Fang, X.; Liu, J.; Wang, M.; Shen, C.; Long, K. Durability of Solidified Sludge with Composite Rapid Soil Stabilizer under Wetting-Drying Cycles. *Case Stud. Constr. Mater.* **2022**, *17*, e01374. [[CrossRef](#)]
2. Liu, L.; Deng, T.; Deng, Y.; Zhan, L.; Horpibulsuk, S.; Wang, Q. Stabilization Nature and Unified Strength Characterization for Cement-Based Stabilized Soils. *Constr. Build. Mater.* **2022**, *336*, 127544. [[CrossRef](#)]

3. Pu, S.; Zhu, Z.; Wang, H.; Song, W.; Wei, R. Mechanical Characteristics and Water Stability of Silt Solidified by Incorporating Lime, Lime and Cement Mixture, and SEU-2 Binder. *Constr. Build. Mater.* **2019**, *214*, 111–120. [[CrossRef](#)]
4. Zhang, T.; Liu, S.; Zhan, H.; Ma, C.; Cai, G. Durability of Silty Soil Stabilized with Recycled Lignin for Sustainable Engineering Materials. *J. Clean. Prod.* **2020**, *248*, 119293. [[CrossRef](#)]
5. Durante Ingunza, M.P.; de Araujo Pereira, K.L.; dos Santos Junior, O.F. Use of Sludge Ash as a Stabilizing Additive in Soil-Cement Mixtures for Use in Road Pavements. *J. Mater. Civ. Eng.* **2015**, *27*, 06014027. [[CrossRef](#)]
6. Tran, K.Q.; Satomi, T.; Takahashi, H. Improvement of Mechanical Behavior of Cemented Soil Reinforced with Waste Cornsilk Fibers. *Constr. Build. Mater.* **2018**, *178*, 204–210. [[CrossRef](#)]
7. Reddy, B.V. Stabilised Soil Blocks for Structural Masonry in Earth Construction. In *Modern Earth Buildings*; Woodhead Publishing: Sawston, UK, 2012; pp. 324–363. ISBN 978-0-85709-616-6.
8. Zhao, Y.; Yang, Y.; Ling, X.; Gong, W.; Li, G.; Su, L. Dynamic Behavior of Natural Sand Soils and Fiber Reinforced Soils in Heavy-Haul Railway Embankment under Multistage Cyclic Loading. *Transp. Geotech.* **2021**, *28*, 100507. [[CrossRef](#)]
9. Liu, C.; Lv, Y.; Yu, X.; Wu, X. Effects of Freeze-Thaw Cycles on the Unconfined Compressive Strength of Straw Fiber-Reinforced Soil. *Geotext. Geomembr.* **2020**, *48*, 581–590. [[CrossRef](#)]
10. Jiang, H.; Cai, Y.; Liu, J. Engineering Properties of Soils Reinforced by Short Discrete Polypropylene Fiber. *J. Mater. Civ. Eng.* **2010**, *22*, 1315–1322. [[CrossRef](#)]
11. Zhao, F.; Zheng, Y. Shear Strength Behavior of Fiber-Reinforced Soil: Experimental Investigation and Prediction Model. *Int. J. Geomech.* **2022**, *22*, 04022146. [[CrossRef](#)]
12. Tiwari, N.; Satyam, N.; Singh, K. Effect of Curing on Micro-Physical Performance of Polypropylene Fiber Reinforced and Silica Fume Stabilized Expansive Soil under Freezing Thawing Cycles. *Sci. Rep.* **2020**, *10*, 7624. [[CrossRef](#)]
13. Akbari, H.R.; Sharafi, H.; Goodarzi, A.R. Effect of Polypropylene Fiber and Nano-Zeolite on Stabilized Soft Soil under Wet-Dry Cycles. *Geotext. Geomembr.* **2021**, *49*, 1470–1482. [[CrossRef](#)]
14. Aryal, S.; Kolay, P.K. Long-Term Durability of Ordinary Portland Cement and Polypropylene Fibre Stabilized Kaolin Soil Using Wetting–Drying and Freezing–Thawing Test. *Int. J. Geosynth. Ground Eng.* **2020**, *6*, 1–15. [[CrossRef](#)]
15. Tan, T.; Huat, B.B.K.; Anggraini, V.; Shukla, S.K.; Nahazanan, H. Strength Behavior of Fly Ash-Stabilized Soil Reinforced with Coir Fibers in Alkaline Environment. *J. Nat. Fibers* **2021**, *18*, 1556–1569. [[CrossRef](#)]
16. Qiu, R.; Tong, H.; Gu, M.; Yuan, J. Strength and Micromechanism Analysis of Microbial Solidified Sand with Carbon Fiber. *Adv. Civ. Eng.* **2020**, *2020*, 8876617. [[CrossRef](#)]
17. Gobinath, R.; Akinwumi, I.I.; Afolayan, O.D.; Karthikeyan, S.; Manojkumar, M.; Gowtham, S.; Manikandan, A. Banana Fibre-Reinforcement of a Soil Stabilized with Sodium Silicate. *Silicon* **2020**, *12*, 357–363. [[CrossRef](#)]
18. Cao, Z.; Ma, Q.; Wang, H. Effect of Basalt Fiber Addition on Static-Dynamic Mechanical Behaviors and Microstructure of Stabilized Soil Compositing Cement and Fly Ash. *Adv. Civ. Eng.* **2019**, *2019*, 8214534. [[CrossRef](#)]
19. Hu, Z.; Wang, Y.; Wang, C. Study on Mechanical Properties of Dredged Silt Stabilized with Cement and Reinforced with Alginate Fibers. *Case Stud. Constr. Mater.* **2023**, *18*, e01977. [[CrossRef](#)]
20. Zhang, M.; Na, M.; Yang, Z.; Shi, Y.; Guerrieri, M.; Pan, Z. Study on Mechanical Properties and Solidification Mechanism of Stabilized Dredged Materials with Recycled GFRP Fibre Reinforced Geopolymer. *Case Stud. Constr. Mater.* **2022**, *17*, e01187. [[CrossRef](#)]
21. *ASTM Standard D854-14*; Standard Test Methods for Specific Gravity of Soil Solids by Water Pycnometer. American Society for Testing and Materials: West Conshohocken, PA, USA, 2014.
22. *ASTM Standard D4318-17*; Standard Test Methods for Liquid Limit, Plastic Limit, and Plasticity Index of Soils. American Society for Testing and Materials: West Conshohocken, PA, USA, 2018.
23. *ASTM Standard D2216-19*; Standard Test Methods for Laboratory Determination of Water (Moisture) Content of Soil and Rock by Mass. American Society for Testing and Materials: West Conshohocken, PA, USA, 2019.
24. *ASTM Standard D7263-21*; Standard Test Methods for Laboratory Determination of Density and Unit Weight of Soil Specimens. American Society for Testing and Materials: West Conshohocken, PA, USA, 2021.
25. *ASTM Standard D2487-17e1*; Standard Practice for Classification of Soils for Engineering Purposes (Unified Soil Classification System). American Society for Testing and Materials: West Conshohocken, PA, USA, 2020.
26. *ASTM Standard D3080-04*; Standard Test Method for Direct Shear Test of Soils Under Consolidated Drained Conditions. American Society for Testing and Materials: West Conshohocken, PA, USA, 2012.
27. *ASTM Standard D2435-04*; Standard Test Methods for One-Dimensional Consolidation Properties of Soils Using Incremental Loading. American Society for Testing and Materials: West Conshohocken, PA, USA, 2011.
28. Gowthaman, S.; Nakashima, K.; Kawasaki, S. Freeze-Thaw Durability and Shear Responses of Cemented Slope Soil Treated by Microbial Induced Carbonate Precipitation. *Soils Found.* **2020**, *60*, 840–855. [[CrossRef](#)]
29. Nafisi, A.; Montoya, B.M.; Evans, T.M. Shear Strength Envelopes of Biocemented Sands with Varying Particle Size and Cementation Level. *J. Geotech. Geoenviron. Eng.* **2020**, *146*, 04020002. [[CrossRef](#)]
30. Samantasinghar, S.; Singh, S.P. Strength and Durability of Granular Soil Stabilized with FA-GGBS Geopolymer. *J. Mater. Civ. Eng.* **2021**, *33*, 06021003. [[CrossRef](#)]
31. Yang, X.; Liang, S.; Hou, Z.; Feng, D.; Xiao, Y.; Zhou, S. Experimental Study on Strength of Polypropylene Fiber Reinforced Cemented Silt Soil. *Appl. Sci.* **2022**, *12*, 8318. [[CrossRef](#)]

32. Liang, S.; Xiao, X.; Fang, C.; Feng, D.; Wang, Y. Experimental Study on the Mechanical Properties and Disintegration Resistance of Microbially Solidified Granite Residual Soil. *Crystals* **2022**, *12*, 132. [[CrossRef](#)]
33. Jose, A.; Kasthurba, A.K. Laterite Soil-Cement Blocks Modified Using Natural Rubber Latex: Assessment of Its Properties and Performance. *Constr. Build. Mater.* **2021**, *273*, 121991. [[CrossRef](#)]
34. Zhang, L.; Gustaysen, A.; Jelle, B.P.; Yang, L.; Gao, T.; Wang, Y. Thermal Conductivity of Cement Stabilized Earth Blocks. *Constr. Build. Mater.* **2017**, *151*, 504–511. [[CrossRef](#)]
35. Deng, Y.; Jiang, Y.; Wu, J.; Sun, H.; Geng, X. Desert Silty Sand Modified by Anionic PAM and Ordinary Portland Cement: Microfabric Reinforcement and Durability. *Transp. Geotech.* **2022**, *37*, 100846. [[CrossRef](#)]
36. Zhang, G.; Ding, Z.; Zhang, R.; Chen, C.; Fu, G.; Luo, X.; Wang, Y.; Zhang, C. Combined Utilization of Construction and Demolition Waste and Propylene Fiber in Cement-Stabilized Soil. *Buildings* **2022**, *12*, 350. [[CrossRef](#)]
37. Hongzhou, Z.; Limei, T.; Shuang, W.; Yanhong, Q. Experimental Study on Engineering Properties of Fiber-Stabilized Carbide-Slag-Solidified Soil. *PLoS ONE* **2022**, *17*, e0266732. [[CrossRef](#)]
38. Sun, J.; Aslani, F.; Lu, J.; Wang, L.; Huang, Y.; Ma, G. Fibre-Reinforced Lightweight Engineered Cementitious Composites for 3D Concrete Printing. *Ceram. Int.* **2021**, *47*, 27107–27121. [[CrossRef](#)]

Disclaimer/Publisher’s Note: The statements, opinions and data contained in all publications are solely those of the individual author(s) and contributor(s) and not of MDPI and/or the editor(s). MDPI and/or the editor(s) disclaim responsibility for any injury to people or property resulting from any ideas, methods, instructions or products referred to in the content.